

39

THE RELATION BETWEEN TOOL GEOMETRY AND THE TAYLOR TOOL LIFE CONSTANT

W. S. LAU*, P. K. VENUVINOD† and C. RUBENSTEIN‡

(Received 21 March 1979; in final form 15 October 1979)

Abstract – In an earlier publication, a relation between tool geometry i.e. rake angle α and clearance angle β and Taylor Constant was proposed and the experiments performed provided data which agreed well with the effect of β but not with that of α . A semi-analytical model is developed here which tries to incorporate the effect of α on the mean temperature at the flank wear land by expressing the relevant relationship in a linear form. Further, it is shown that flank wear is to be considered as a combination of "lump" and "layer" types of wear. The relatively unused method of high speed steel-mild steel tool-work thermocouple technique is successfully used to obtain temperature data. The experimental results agree well with the model.

INTRODUCTION

THE ROLE of Taylor's equation in the determination of the economics of machining is well known. The index n and constant C of Taylor's Tool Life equation ($VT^n = C$) are the parameters through which cutting tool material and the tool geometry influence the cost of machining and machining rates. A review of relevant literature indicates that the magnitudes of n and C have generally been determined empirically. While there are a number of models proposed for describing the wear of tool flank, it is only recently [1, 2] that an attempt has been made to relate, analytically, cutting tool geometry to Taylor constant C . It has been shown, [2] that

$$C \propto [(\cot \beta - \tan \alpha)^n F(\alpha, \beta)^{1/\varepsilon}]^{-1}, \quad (1)$$

where

α is the rake angle,

β is the clearance angle,

$F(\alpha, \beta)$ is a suitable function of α and β

and

ε is the index of cutting speed V when the mean flank temperature.

θ_f is related to it by the equation $\theta_f = \text{const } V^\varepsilon$.

Experiments showed excellent correlation with equation (1) when only the clearance angle β was varied [2]. When the rake angle α was varied, however, correlation was not so good, indicating that $F(\alpha, \beta)$ was strongly dependent on α . The present paper is the result of an attempt at providing a greater understanding of $F(\alpha, \beta)$ and thereby of the relationship between rake angle and Taylor constant. The work depends basically on the earlier model [1] but tries to include the effect of rake angle on the mean flank temperature θ_f .

DESCRIPTION OF TOOL WEAR MODEL

A model for the flank wear of cutting tools is now developed starting from the assumptions made in Ref. [1].

* Senior Lecturer, Department of Production & Industrial Engineering, Hong Kong Polytechnic, Hung Hom, Kowloon, Hong Kong.

† Senior Lecturer, Department of Production & Industrial Engineering, Hong Kong Polytechnic, Hung Hom, Kowloon, Hong Kong.

‡ Professor, Department of Mechanical Engineering, Ben Gurion University of the Negev, P.O.B. 653, Beer Sheva, Israel.

Currently: Senior Visiting Research Fellow, Department of Mechanical Engineering, U.M.I.S.T., Manchester.

- (i) Over the surface of the flank wear land of length l_f and width W , a mean pressure, p_m , and a representative temperature, θ_f , can be defined.
- (ii) Contact between the flank face of the tool and the machined surface occurs over n_o asperities per unit apparent area of contact.
- (iii) All asperity contacts are circular and of radius r_o when the tool and the workpiece are in contact under a pure normal load, L , the normal load occurring during cutting (see equation 5 below).
- (iv) The volume of a wear particle is given by $k_1 r^2 h$ where r is the radius of the wear particle, h is its height and k_1 is a factor depending on its shape.
- (v) The radius r may be expressed as gr_o where g is a factor depending on the degree of adhesion and ductility of the deforming asperity.
- (vi) The height h is proportional to the radius r and is given by

$$h \simeq h_1 \frac{r}{V}, \quad (2)$$

where V is the cutting speed [1].

The rate of volume wear at the tool flank, Q , may be expressed [1] as

$$Q = \frac{c_1 k_1}{\pi} p g^2 h_1 W l_f \frac{H_m}{H}, \quad (3)$$

where H_m is the workpiece hardness,

H is the hardness of the deforming asperities,

$$c_1 = p_m / H_m,$$

and p is the probability of a wear particle forming when a junction is broken.

The factor $g^2 h_1$ may be related to the properties of the work material [1] as

$$g^2 h_1 = R_o^a \sigma_o^b \theta_f^e h_1, \quad (4)$$

where R_o and σ_o are the percentage reduction and degree of adhesion of the deforming asperities at room temperature θ_o and a, b, e are suitable constants.

The normal load L on the flank wear land is given by

$$L = p_m W l_f. \quad (5)$$

The hardness of the asperities H may be related to temperature θ_f [1] as

$$H = H_o \left(\frac{\theta_f}{\theta_o} \right)^{-g_1}, \quad (6)$$

where H_o is the tool hardness at temperature θ_o and g_1 is a suitable constant.

Combining equations (3)–(6),

$$Q = K_1 \theta_f^q L, \quad (7)$$

where

$$K_1 = \frac{k_1 R_o^a \sigma_o^b h_1 p}{\pi \theta_o^{g_1} H_o}$$

and

$$q = e + g_1.$$

Equation (7) agrees with Archard's result [3], only if θ_f is constant or, if not constant, if the wear mechanism is temperature independent. There it was shown that, for "lump" wear, wear rate is proportional to load. In "lump" wear, the depth to which the material is torn at each asperity is proportional to r_o . This is equivalent to the condition $h \propto r_o$ assumed in the foregoing analysis.

Archard [3] also presents an analysis of the condition of "layer" type removal, the definition of which is that the depth of torn material is independent of r_o and shows that

$$Q \propto L^{0.75}. \quad (8)$$

Little experimental evidence is available today to attribute flank wear of cutting tools to either "lump" or "layer" type of wear. In the later part of this paper, however, it will be demonstrated that an assumption of pure "lump" type of wear leads to a discrepancy when compared to experimental observations. It is therefore proposed to assume that flank wear occurs as a result of a combination of "lump" and "layer" types of wear. This condition may be accommodated by modifying equation (7) as

$$Q = K'_1 \theta_f^q L^\omega, \quad (9)$$

where

ω may take a value lying in the range 0.75 (for pure "layer" type) to 1 (for pure "lump" type).

and

K'_1, q' are modified constants to take into account the changed conditions of wear.

It has been shown in [1] that Q is related to the rake angle α and clearance angle β as

$$Q = \frac{Wl_f}{(\cot \beta - \tan \alpha)} \frac{dl_f}{dt}. \quad (10)$$

The temperature on the flank face is related to the mean temperature at the chip tool contact area θ_r [4]. For a given value of l_f , θ_r may be expressed in terms of workpiece hardness H_m , cutting speed V and feed f as

$$\theta_r \propto H_m^p V^\varepsilon f^\eta W^\gamma. \quad (11)$$

Assuming, $\theta_f \propto \theta_r$ and including the effect of l_f on θ_f [1],

$$\theta_f = K H_m^p V^\varepsilon f^\eta W^\gamma l_f^\delta \quad (12)$$

where $K, p, \varepsilon, \eta, \gamma$ and δ are suitable constants.

An expression for the rate of flank wear may now be obtained by combining equations (5), (9), (10) and (12).

$$\frac{dl_f}{dt} = K'_1 K^q H_m^{pq} f^{\eta q} W^{\gamma q} l_f^{\omega q} p_m^{\omega} l_f^{\delta q} V^{\eta q} (\cot \beta - \tan \alpha). \quad (13)$$

It is easy to demonstrate that at $\omega = 1$ ("lump" removal), this equation reduces to the equation for wear rate proposed in reference [1]. However, when $\omega = 1$, equation (13) indicates an increasing rate of wear dl_f/dt as l_f increases. This is contrary to the known nature of wear curves where, generally, the curve l_f against time is either straight or convex towards the time axis (see Fig. 1) in the steady state wear zone. This condition can only exist when $\omega < 1$. This justifies the assumption of combined "layer" and "lump" wear.

In Fig. 1 the onset of the secondary, "steady-state" wear region is shown as occurring at $l_f = l_1$ and its termination at $l_f = l_2$. Assuming that l_1 is small compared to the tool life criterion $l_f = l_o$, we can integrate using the boundary conditions $l_f = 0$ at $t = 0$ and $l_f = l_o$ at $t = T$ (tool life) and then compare the resulting equation with the Taylor Tool Life equation

$$V T^n = C. \quad (14)$$

It can be seen that

$$q' n \varepsilon = 1 \quad (15)$$

and

$$C = \frac{l_o^{(2-\omega-\delta q')n} (\cot \beta - \tan \alpha)^{-n}}{K'_1 K^{q'n} H_m^{pq'n} f^{\eta q'n} W^{(\gamma q'+\omega-1)n} p_m^{\omega n}}. \quad (16)$$

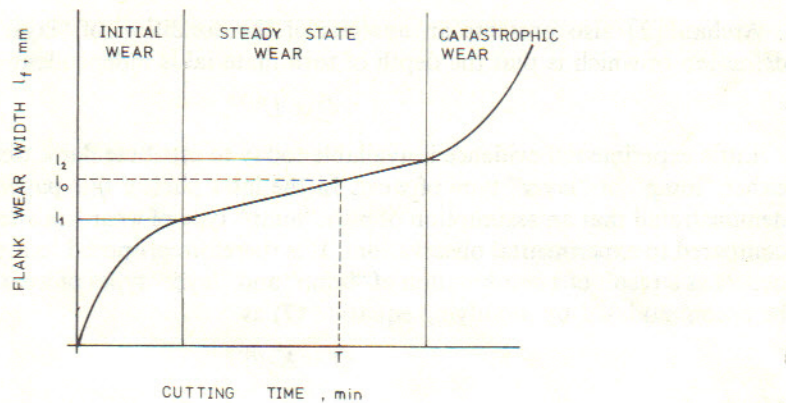


FIG. 1. Typical tool wear curve.

Following the procedure given in [1], it can be shown that q' in the above equation is equivalent to the index of cutting temperature in Schaumann-Schallbroch equation [5]. Thus,

$$T\theta_r^{q'} = \text{Constant.} \quad (17)$$

If it is assumed that the factors other than $(\cot \beta - \tan \alpha)$ are constant, one has

$$C\alpha(\cot \beta - \tan \alpha)^{-n}. \quad (18)$$

Figures 2(a), (b) and (c) show the results obtained from tests on machining mild steel with H.S.S. tools with β varying from 2 to 20° and with $\alpha = 10^\circ$ [2]. It is seen that the correlation with equation (16) is excellent. However, the index n obtained from equation (18) is 0.35 whereas the index of n as observed from the relationship between V and T for the same data (see Fig. 3) was 0.41. Fig. 3 includes the results obtained by varying rake angle α in the range $10-30^\circ$ at higher cutting speeds with air as cutting fluid. It is seen that there is no agreement with equation (18) in this case. This indicates that the rake angle has a strong influence on factors other than $(\cot \beta - \tan \alpha)$ in equation (16). $F(\alpha, \beta)$ in equation (1) is thus largely a function only of α . The nature of this function is examined in the next section.

INFLUENCE OF RAKE ANGLE

The foregoing analysis is based on the assumption that, at a given cutting speed, the flank temperature θ_f and normal pressure $p_m = c_1 H_m$ are constant, irrespective of rake and clearance angles. A little thought shows that this assumption is reasonable for varying clearance angles within a limited range. However, as is well known, a variation in rake angle causes a significant change in the mean temperature at the rake face θ_r . Figure 4 shows a typical relationship between θ_r and α [6]. It appears that, within the range of rake angles wherein the rate of decrease of rake face temperature with rake angle is relatively slow, the relationship can be expressed by a linear expression of the form.

$$\theta_r = \theta_{r0}(1 - m_1 \alpha), \quad (19)$$

where θ_{r0} is the magnitude of θ_r when $\alpha = 0$ and m_1 is a suitable positive constant.

In addition, an increase in rake angle reduces the path of conduction of heat from the rake to the flank surface. The exact nature of this effect is unknown and no information is available in the literature in connection with this aspect. It will be assumed, for the sake of simplicity, that a linear relation between θ_r and θ_f exists for a given tool geometry. Thus, for a fixed clearance angle, it will be assumed that

$$\theta_f = A_1 \theta_r(1 + m_2 \alpha), \quad (20)$$

where A_1 and m_2 are suitable positive constants.

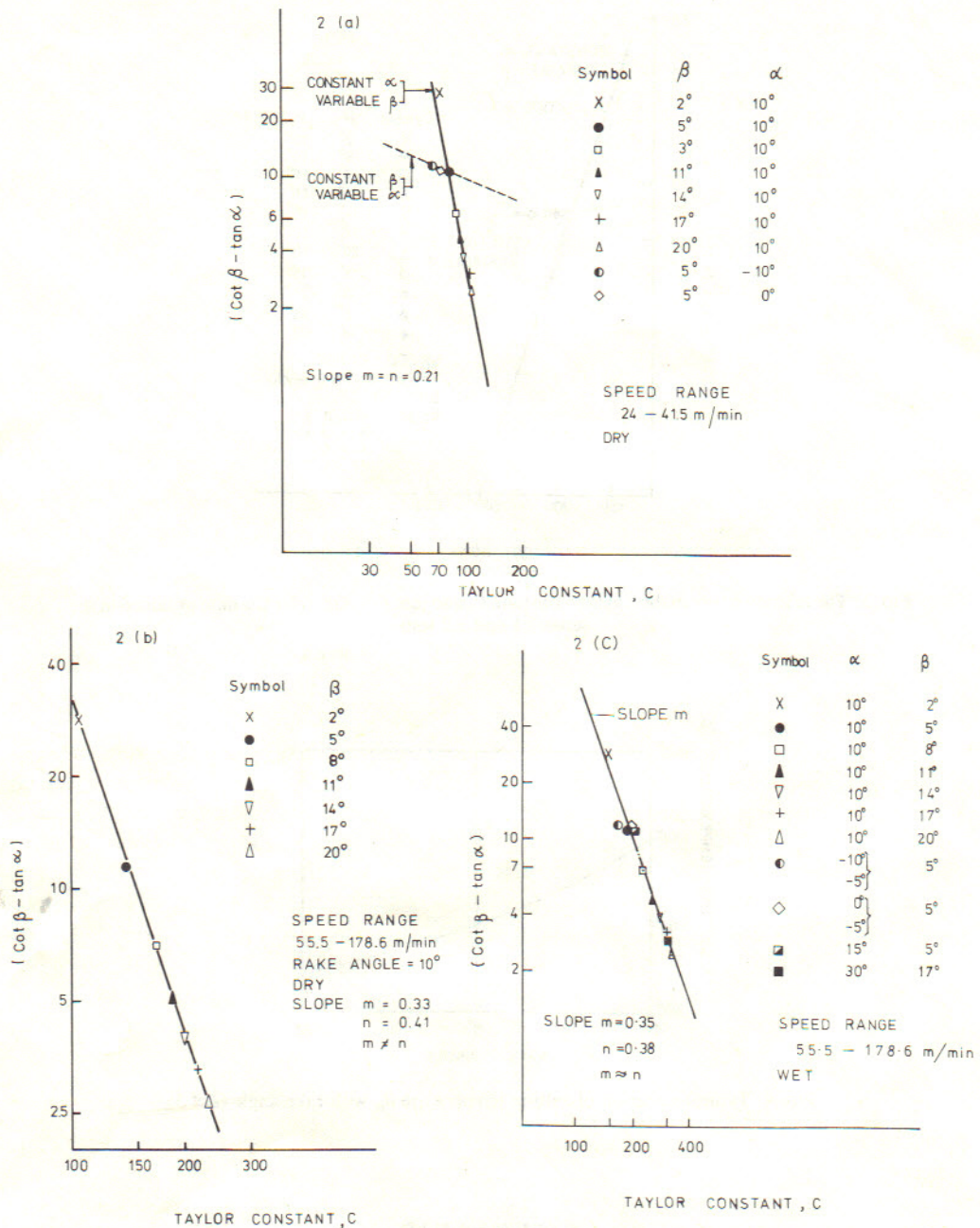


FIG. 2. The relation between the Taylor Constant, C, and $(\cot \beta - \tan \alpha)$ for the data obtained (a) in series 1.1 and 1.2 tests, (b) in series 2.1 test, (c) in series 3.1 and 3.2 tests.

In view of the above factors equation (12) now takes the form

$$\theta_f = KVef^{\eta} l_f^{\delta} W^{\gamma} H_m^p A_1 \theta_{ro} (1 - m_1 \alpha) (1 + m_2 \alpha). \quad (21)$$

Proceeding as before one has the following equation in place of equation (18)

$$C \propto [(\cot \beta - \tan \alpha) \{ (1 - m_1 \alpha) (1 + m_2 \alpha) \}^{1/n \varepsilon}]^{-n}. \quad (22)$$

Experimental studies show that the magnitudes of m_1 and m_2 are small so that the term $(1 - m_1 \alpha) (1 + m_2 \alpha)$ in the above equation can be replaced by $(1 - m^* \alpha)$, where $m^* = (m_1 - m_2)$, without significant error, so that

$$C \propto [(\cot \beta - \tan \alpha) (1 - m^* \alpha)^{1/n \varepsilon}]^{-n}. \quad (23)$$

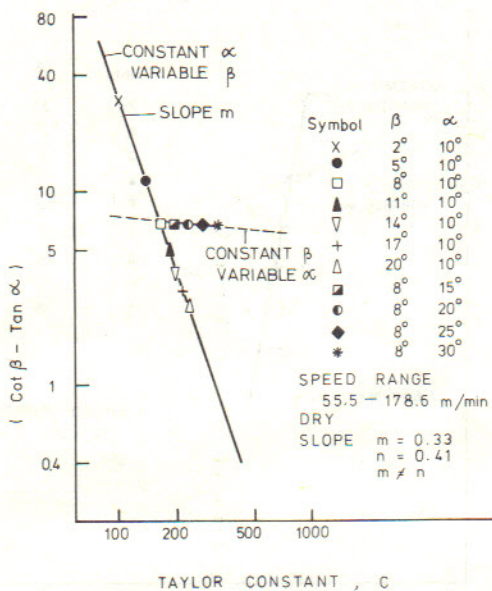


FIG. 3. The relation between the Taylor Constant, C, and $(\cot \beta - \tan \alpha)$ for the data obtained in the series 2.1 and 2.2 tests.

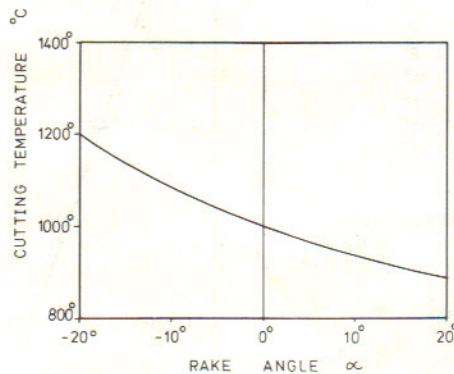


FIG. 4. Typical variation of cutting temperature θ_m with rake angle (Ref 5).

EXPERIMENTS

Experiments were conducted to test equation (23) on annealed mild steel tubes (50.8 mm O.D., 2 mm wall thickness). The chemical composition of the specimens was 0.2% C, 0.17% Si, 0.89% Mn, 0.064% S and 0.015% P (hardness BHN115). Specimens from one production batch were cut orthogonally on a Colchester Triumph 2000 centre lathe at a constant feed of 0.1016 mm/rev. The cutting tool material was MTM 41 high speed steel (hardness Rc65; composition 0.8% C, 6.4% W, 4.3% Cr, 1.9% V, 5% MO), all of which were obtained from the same production batch and were mounted in the same tool holder when used for the cutting tests. The tool life criterion, $l_f = l_o$ adopted for all the tests was a flank wear land of 0.18 mm, this value having been chosen so that for all the tests performed, the condition

$$l_1 \ll l_o < l_2$$

was obeyed (Fig. 1) i.e. it was ensured that in all cases l_o fell in the range of steady state wear.

Three series of cutting tests were performed. Table 1 gives the details of the test conditions. Flank wear land was measured using a tool maker's microscope. A tool-workpiece

and the corresponding cutting conditions. It is the intention to publish a detailed description of the apparatus and technique used in the experiments in a separate paper. The results of the present work are, however, summarized in Table I.

It is evident from the table that the cutting conditions adopted in the present work are not the same as those used by D. L. Taylor in his original experiments. The cutting conditions adopted in the present work are, however, similar to those used by D. L. Taylor in his experiments on the effect of tool geometry on the Taylor tool life constant.

The cutting conditions adopted in the present work are, however, not the same as those used by D. L. Taylor in his original experiments. The cutting conditions adopted in the present work are, however, similar to those used by D. L. Taylor in his experiments on the effect of tool geometry on the Taylor tool life constant.

The cutting conditions adopted in the present work are, however, not the same as those used by D. L. Taylor in his original experiments. The cutting conditions adopted in the present work are, however, similar to those used by D. L. Taylor in his experiments on the effect of tool geometry on the Taylor tool life constant.

The cutting conditions adopted in the present work are, however, not the same as those used by D. L. Taylor in his original experiments. The cutting conditions adopted in the present work are, however, similar to those used by D. L. Taylor in his experiments on the effect of tool geometry on the Taylor tool life constant.

The cutting conditions adopted in the present work are, however, not the same as those used by D. L. Taylor in his original experiments. The cutting conditions adopted in the present work are, however, similar to those used by D. L. Taylor in his experiments on the effect of tool geometry on the Taylor tool life constant.

The cutting conditions adopted in the present work are, however, not the same as those used by D. L. Taylor in his original experiments. The cutting conditions adopted in the present work are, however, similar to those used by D. L. Taylor in his experiments on the effect of tool geometry on the Taylor tool life constant.

The cutting conditions adopted in the present work are, however, not the same as those used by D. L. Taylor in his original experiments. The cutting conditions adopted in the present work are, however, similar to those used by D. L. Taylor in his experiments on the effect of tool geometry on the Taylor tool life constant.

TABLE I. THE CUTTING CONDITIONS ADOPTED IN THE PRESENT WORK

Test series	1.1	1.2	2.1	2.2	3.1	3.2
Rake angle	constant at 5°	$-10^\circ, 0^\circ, 10^\circ$	constant at 10°	$0^\circ, 5^\circ, 15^\circ$	constant at 10°	$-10^\circ, -5^\circ, 0^\circ, 5^\circ, 15^\circ$
Clearance angle	$2^\circ-20^\circ$ at 3° intervals	constants at 5°	$2^\circ-20^\circ$ at 3° intervals	constant at 5°	$2^\circ-20^\circ$ at 3° intervals	constant at 5°
Cutting fluid	air	air	air	air	Drommus B	Drommus B
Speed range in m/min	24-41.5	24-41.5	55.5-178.6	55.5-178.6	55.5-178.6	55.5-178.6

Drommus is a trade name registered to Shell Chemical Co. Ltd.

thermocouple technique was used to obtain a measure of the cutting temperature θ_m . The measurement was made using a Keithley 616 digital Electrometer. The tool holder was insulated from the machine. The positive lead of the electrometer was connected to the tool while the negative lead was connected to the rear end of the spindle through a graphite/copper brush. Care was taken to check that there was no parasitic e.m.f. at the brush. The signals from the dynamometer and the electrometer were recorded on a SE 3006/DL u.v. recorder. The temperature θ_p at the junction of the tool and the tool holder was monitored by a portable digital thermocouple unit.

The calibration of the h.s.s.-mild steel thermocouple was made using the silver bead technique. The tool and a long specimen of the work material were inserted in a silver bead placed in a crucible. The temperature of the bead was varied either by heating on a burner or by cooling from a molten state. The bead temperature was monitored by the digital thermocouple. The thermo-e.m.f. was measured using the Electrometer. Parasitic voltages at the junctions of the leads with the tool and the work-specimen were avoided by directing compressed air jets onto the junctions.

All signals were recorded on the u.v. recorder. A similar technique was used to calibrate the parasitic e.m.f. generated between the tool holder and the tool. In this case, the tool holder replaced the work specimen.

RESULTS AND DISCUSSION

Figure 5 shows the calibration curve obtained for the high speed steel-mild steel thermocouple. It can be seen that a straight line can be used as a reasonable approximation to the curve in the temperature range 220–660°C. Below 220°C, the output is negative and too small in magnitude to be reliable. Beyond 600°C, there is a tendency for the thermocouple to saturate. The useful range of the thermocouple may thus be taken as 200–650°C, which is satisfactory for the present purpose.

Figure 6 shows the calibration curve obtained for the tool holder-high speed steel thermocouple. Since the parasitic temperatures are much lower than the cutting temperatures, this curve has been obtained only up to 200°C. For a given parasitic temperature θ_p the parasitic e.m.f. e_p can be read directly from this graph.

Figure 7 shows the relationship obtained relating the measured thermo-e.m.f. e_m between the cutting tool and the workpiece to the parasitic temperature θ_p at the middle of the contact region between the tool and the tool holder.

The corrected temperature θ_m can now be obtained from the measured e.m.f. e_m by the following procedure.

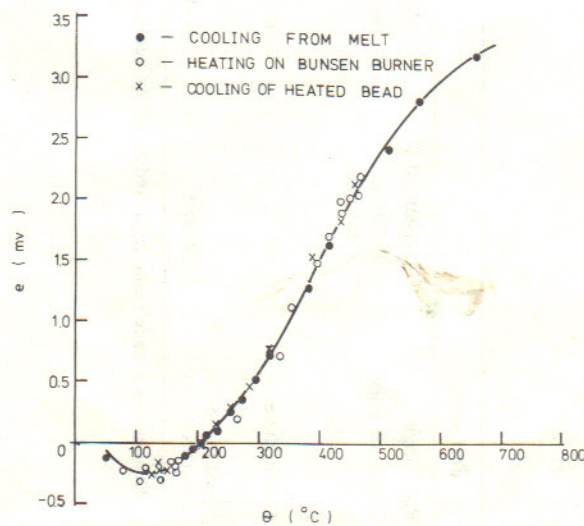


FIG. 5. High speed steel tool-mild steel thermocouple calibration curve.

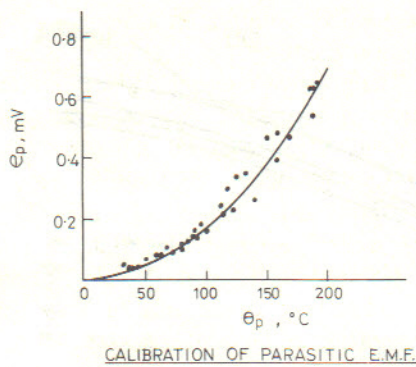


FIG. 6. Tool holder-high speed steel thermocouple calibration curve.

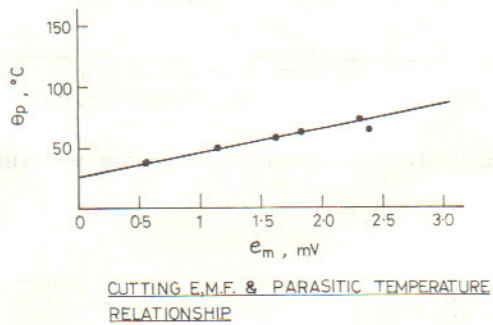


FIG. 7. Relationship between measured e.m.f. and the parasitic temperature occurring at the tool-tool holder contact surface.

- (i) read θ_p on Fig. 7 for the given e_m ;
- (ii) read e_p for the above θ_p on Fig. 6;
- (iii) obtain corrected e.m.f. at the tool tip e from the relationship $e = e_m - e_p$; and
- (iv) obtain the corrected temperature θ_m for the above value of e from Fig. 5.

Figures 8 and 9 show the variation of measured (and corrected) cutting temperature θ_m with cutting speed V in the low and high ranges of rake angles respectively. Curve fitting was done by conducting curvilinear regression analysis using a polynomial function. Inclusion of terms up to the second degree was found adequate. The errors due to regression analysis were generally lower than the experimental errors. Each curve has been approximated by straight lines in the low and high speed regions. The slopes of the tangent lines at representative speeds give the magnitude of ε in each range and the results are tabulated in Table 2. It is seen from Figs. 8 and 9 that the effect of rake angle on ε is considerably less than the effect due to cutting speed. Consequently, ε can be taken as 0.15 for the high speed range and 0.38 for the low speed range. Takayama and Murata have noted a similar fall in ε at high cutting speeds while machining with carbide tools [7]. An analysis of the data obtained by Zorev [8] while machining steel 20 by a 20A-0 tool also leads to a similar conclusion. The values of ε obtained by Zorev [8] at low and high speed ranges are also practically the same as those obtained from the present investigation.

Figures 10 and 11 show the same data arranged so as to give the relationship between cutting temperature θ_m and rake angle. There is a gradual decrease in θ_m as rake angle increases - see Fig. 4. There is however an unexpected steep fall in θ_m in the range of $\alpha = 30^\circ$. Repeated experiments confirmed this trend. However, for the sake of simplicity, the analysis here is limited to rake angles less than 25° . The data were subjected to the same procedure of regression analysis as used for Figs. 8 and 9. The low rake angle range ($\alpha = -10$ to 10°) and high rake angle range ($\alpha = 10$ — 25°) have been approximated by straight lines given by

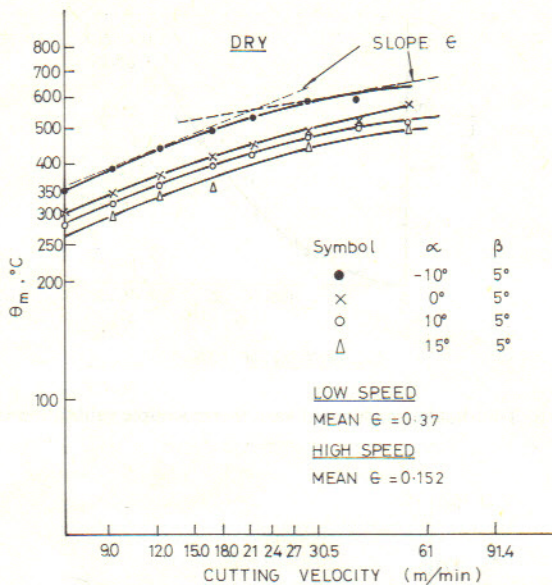


FIG. 8. Variation of measured cutting temperature θ_m with cutting speed in the low rake angle range.

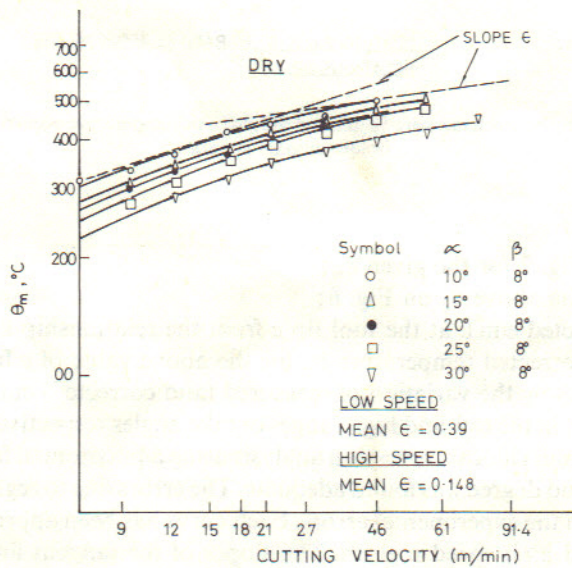


FIG. 9. Variation of measured cutting temperature θ_m with cutting speed in the high rake angle range.

tangents at $\alpha = 0$ and 20° . The slopes of these straight lines when divided by the intercept on θ_m -axis give the values of m_1 (see equation 19). The results are tabulated in Table 2. The magnitude of m_1 can be taken as 0.011 for the low rake range and 0.0082 for the high rake range.

Figures 12(a) and (b) show the observed $V-T$ relationships at different rake angles. The results of linear regression analysis are summarised in Table 2. It is seen that Taylor's Equation is generally obeyed. The magnitude of index n , however, is found to be 0.21 in the low speed range and 0.41 in the high speed range. A similar increase in n with cutting speed V has been reported by Zorev [9] while machining with carbide tools. An explanation for this phenomenon is now given.

	0	1.1 and 1.2	Test series 2.1 and 2.2	3.1 and 3.2
Mean ε (Figs. 8 and 9)	0.38	0.15	—	—
Mean q		15.9	—	—
m_1 (Figs. 10 and 11)	0.011	0.0082	—	—
m^*	0.003	0.0055	0.002	—
$m_2 = m_1 - m^*$	0.008	0.0027	—	—
n from Tool life curve (Figs. 12a, b)	0.21	0.41	0.38	—
n from equation (23)	0.18	0.40	0.34	—

TABLE 2. THE EXPERIMENTALLY DETERMINED VALUES OF THE PARAMETERS ε , q , m_1 , m_2 , m^*
AND TWO ESTIMATES OF n

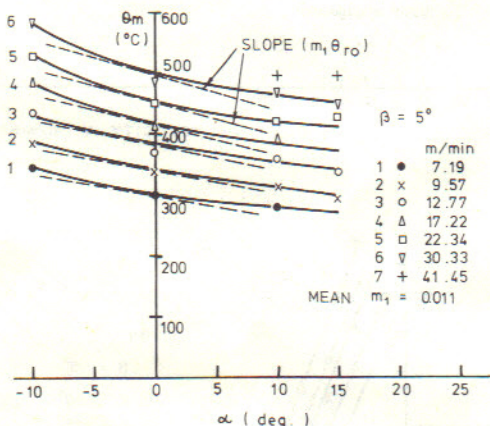


FIG. 10. The relationship between cutting temperature θ_m and rake angle at rake angles from -10° to 15° .

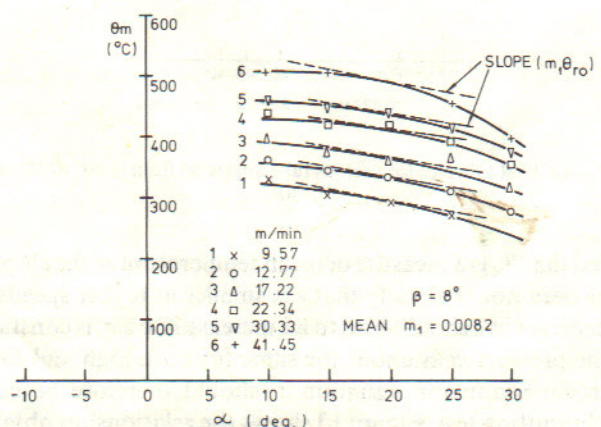


FIG. 11. The relationship between cutting temperature θ_m and rake angle at rake angles from 10° to 30° .

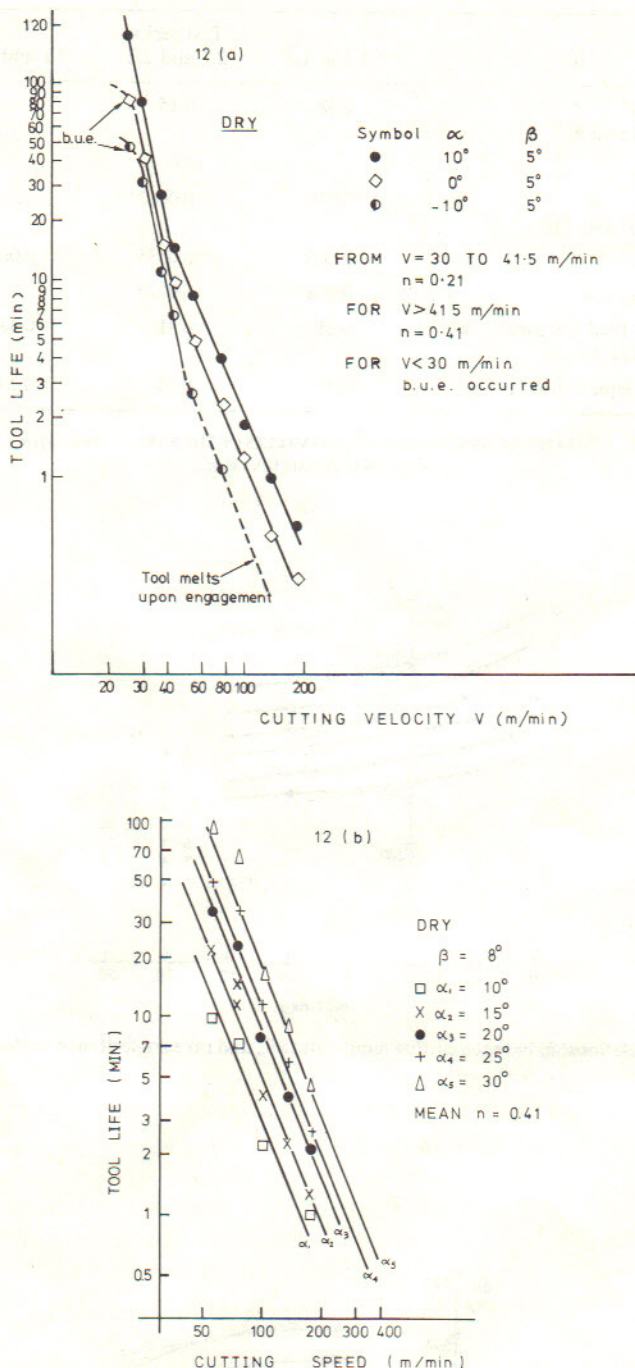
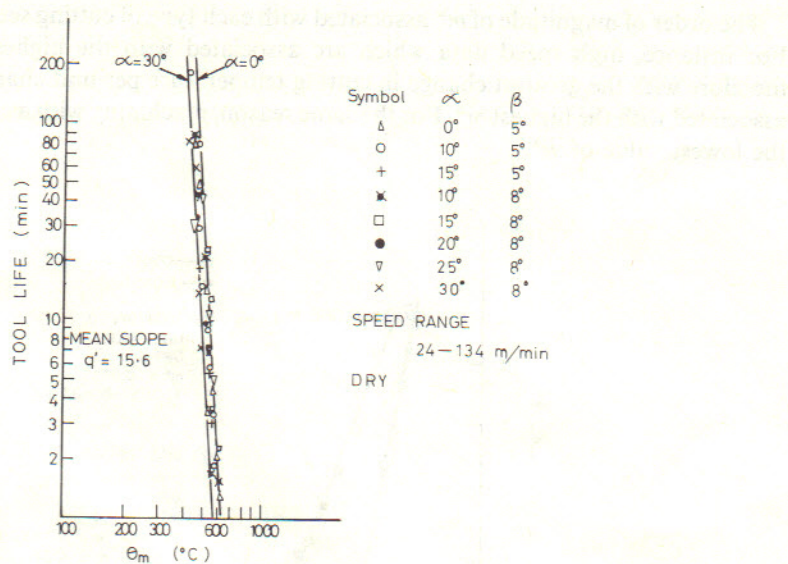


FIG. 12. The Taylor Tool Life plot for various rake angles (a) from -10° to 10° and (b) from 10° to 30° .

Let it be assumed that θ_m is a measure of mean temperature at the chip/tool interface on the rake face θ_r . It has been noted already that ε is smaller at higher speeds. Consequently, and since $q'ne = 1$, a decrease in ε should lead to an increase in n if q' is constant. This is confirmed by the fact that the product ne is about the same for both high and low speed ranges. The index of Schallbroch-Shaumann equation q' should therefore be constant for the data obtained during the cutting test. Figure 13 shows the relationship obtained between θ_m and T . It is seen that the entire data can be expressed by the equation $T\theta_m^{q'} = \text{const}$. Linear regression analysis gives $q' = 15.6$ which agrees well with the mean magnitude of $1/ne = 15.9$.

FIG. 13. Relationship between tool life and cutting temperature θ_m .

At this stage it is possible to speculate about the magnitude of δ . Assuming that the steady state wear curve is a straight line, (i.e. dl_f/dt is independent of l_f), it follows from equation (13) that

$$\delta q' + \omega - 1 \simeq 0. \quad (24)$$

Taking $q' = 15.9$ and the two independent values of ω (0.75 and 1), it is seen that δ lies in the range 0 (for "lump" wear when $\omega = 1$) to 0.0157 (for "layer" wear when $\omega = 0.75$). Since δ cannot be zero or negative, one may conclude again that pure "lump" wear is unlikely to occur at the tool flank. Therefore, some component of "layer" type wear can always be expected. The magnitude of the range of δ calculated above agrees well with the estimated value from the data on cutting temperature at different values of flank wear land obtained by Greenhow and Rubenstein [10].

The magnitude of C is dependent on n , q and m^* as per equation (23). Experimentally, the magnitude of C can be obtained from the $V-T$ relationships at each rake angle. Since the magnitudes of n and q are already known it is possible, in principle, to determine m^* from this data. In fact the magnitude of m^* was obtained separately for the low speed and high speed dry cutting data by trial and error. The magnitudes of m^* for the two ranges of speed were found to be 0.003 and 0.0055 as illustrated in Fig. 14. At these values of m^* the data obtained by varying rake as well as clearance angles fall neatly on the same straight line.

At other values of m^* , it is observed that two separate straight lines respectively are obtained for $\alpha = \text{const}$ and $\beta = \text{const}$ (e.g. see Fig. 3 where $m^* = 0$). It may be noted that the low speed data are usually associated with low rake angles since the tools burn out at higher speeds. Similarly, the high speed data are associated with high rakes. The magnitude of m_2 can be obtained from the difference ($m_1 - m^*$) which gives a value of 0.008 for the low V -low α range and a value of 0.0027 for the high V -high α range. In both cases the magnitude of m_2 is positive as assumed in the development of equation (23).

The slopes of the straight lines in Fig. 14 as obtained by regression analysis give a value of 0.184 in the low V -low α range and a value of 0.4 in the high V -high α range. These agree reasonably well with the Taylor index n obtained for the two ranges, viz. 0.21 and 0.41 respectively.

Figure 15 shows the results of the analysis of data obtained with the application of coolant assuming $q' = 15.9$, $m^* = 0.002$ in this case. The slope of the straight line obtained by regression analysis is 0.34 in this case which agrees well with the value of $n = 0.38$ obtained from the Taylor plot.

The order of magnitude of m^* associated with each type of cutting seems to be reasonable. For instance, high speed data which are associated with the highest temperatures and therefore with the greatest change in cutting temperature per unit change in rake angle are associated with the highest m^* . For the same reason, machining with a cutting fluid produces the lowest value of m^* .

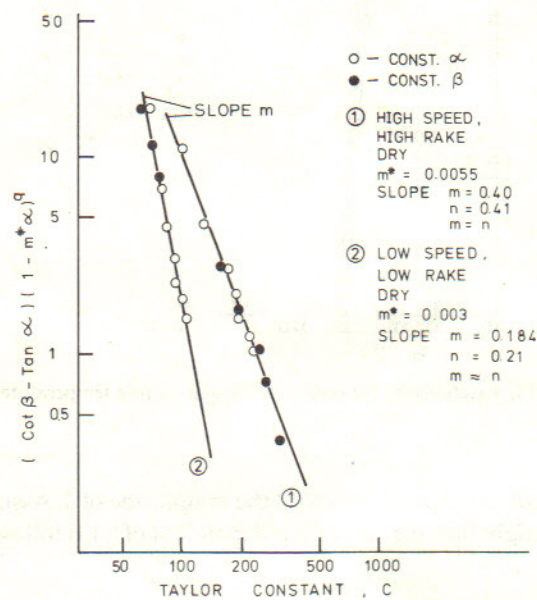


FIG. 14. The relationship between Taylor Constant C, and $[(\cot \beta - \tan \alpha)(1 - m^* \alpha)^{1/m^*}]$ for Test series 1.1, 1.2, 2.1 and 2.2.

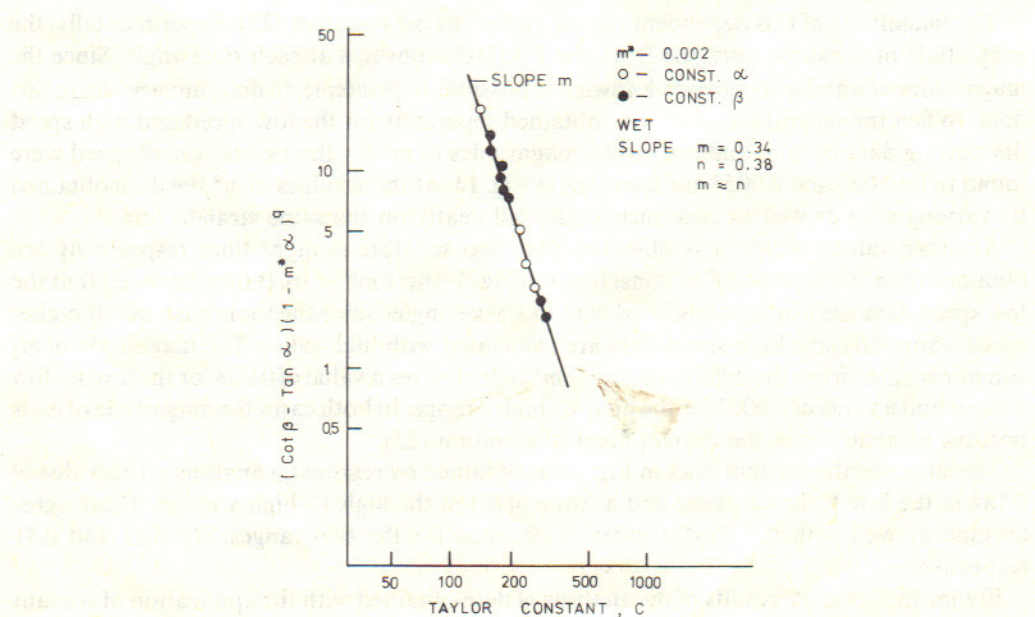


FIG. 15. The relationship between Taylor Constant, C, and $[(\cot \beta - \tan \alpha)(1 - m^* \alpha)^{1/m^*}]$ for Test series 3.1 and 3.2.

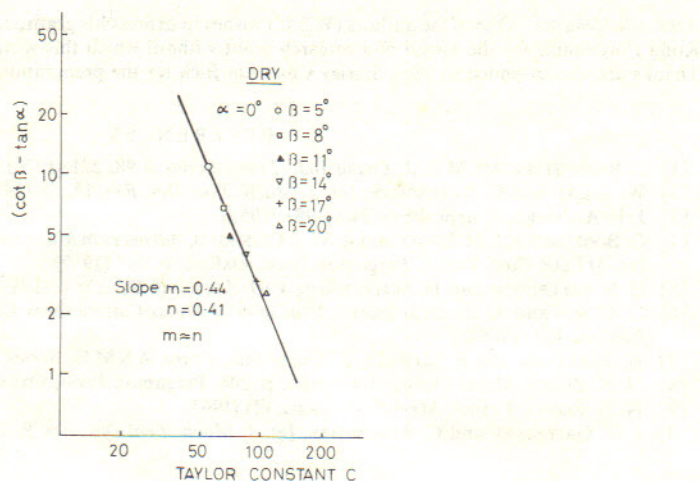


FIG. 16. The relationship between Taylor Constant, C, and $[(\cot \beta - \tan \alpha)(1 - m^* \alpha)^{1/n}]$ at $\alpha = 0^\circ$.

The existence of identical straight lines for constant β and constant α values in Figs. 14 and 15, the observation that the slopes of these straight lines agree well with the corresponding values of Taylor Index n and the observation that the estimated values of m_2 are reasonable and always positive indicate that equation (23) is a reasonable expression of the influence of rake and clearance angles on Taylor Constant C. To test the model further, experiments were conducted specifically with zero rake angle tools. At $\alpha = 0$, equation (23) becomes independent of m^* . Thus, the correlation of equation (23) should be obtained without a need to fit the value of m^* with the results. Figure 16 shows the experimental results with $\alpha = 0$ at different clearance angles. It is seen that the slope of the graph agrees with n .

Further work, however, will be necessary to estimate rigorously the magnitudes of m_2 in different conditions by solving the problem of conduction heat transfer from the tool rake to the tool flank.

CONCLUSIONS

1. The high speed steel-mild steel tool-work thermocouple method is useful in the range of cutting temperatures from 220 to 650°C. The typical calibration curve is as in Fig. 6.
2. Flank wear of cutting tools occurs as a result of a combination of "lump" and "layer" types of wear.
3. In orthogonal cutting of mild steel by high speed steel
 - (a) Taylor exponent n increases from 0.1 to 0.2 at low speeds to 0.41 at high speeds mainly because of the decrease in exponent ϵ of cutting speed V in the relationship $\theta_r = \text{Const } V^\epsilon$. Rake and clearance angles have relatively little effect on the magnitudes of ϵ and n .
 - (b) Schallbroch-Schaumann exponent q' in the relationship $T\theta_m^{q'} = \text{Const}$ remains a constant irrespective of variations in rake angle, clearance and cutting speed within the practical range.
 - (c) Equation (22) is a reasonable expression of the influence of rake and clearance angles on the Taylor Constant. The expression is based on linear approximations of the influence of rake angle on mean chip/tool contact temperature θ_r and on the conduction heat transfer from the rake surface to the flank surface. m_1 and m_2 are the corresponding linear coefficients.
 - (d) The influence of m_1 and m_2 may be combined and expressed by a single coefficient m^* ($= m_1 - m_2$) as in equation (23). The magnitude of m^* is about 0.01 in the low speed-low rake range (dry cutting); about 0.003 in the high speed-high rake range (dry cutting); and 0.002 when Dromnus B cutting oil in water is used as the cutting fluid. Clearance angle has little influence on the magnitude of m^* .

Acknowledgements — One of the authors (W.S.L.) wishes to express his gratitude to the Administrators of the Hong Kong Polytechnic for the award of a research grant without which this work could not have been undertaken. Thanks are also extended to Miss Shirley Chan Lai Bick for the preparation of the manuscript.

REFERENCES

- [1] C. RUBENSTEIN, A.S.M.E. *J. Engng Ind., Trans. Series B* **98**, 221 (1976).
- [2] W. S. LAU and C. RUBENSTEIN, *Int. J. Mach. Tool Des. Res.* **18**, 59 (1978).
- [3] J. F. ARCHARD, *J. appl. Phys.* **24**(8), 981 (1953).
- [4] G. BOOTHROYD, J. M. EAGLE and A. W. J. CHISHOLM, *Advances in Machine Tool Design and Research, Proc. 8th Int. MTDR Conf.* Part 1, Pergamon Press, Oxford, p. 667 (1967).
- [5] H. SCHALLBROCH and H. SCHAUmann, *VDI Zeitschrift* **81**, 325 (1937).
- [6] G. C. SEN and A. BHATTACHARYA, *Principles of Metal Cutting*, New Central Book Agency, Calcutta, 2nd Edition, 400 (1969).
- [7] H. TAKEYAMA and R. MURATA, *J. Engng Ind., Trans. A.S.M.E., Series B* **85**, 33 (1963).
- [8] N. N. ZOREV, *Metal Cutting Mechanics*, p. 248. Pergamon Press, Oxford (1966).
- [9] N. N. ZOREV, *Vestnik Mashinostroyenia*, (2) (1965).
- [10] J. N. GREENHOW and C. RUBENSTEIN, *Int. J. Mach. Tool Des. Res.* **9**, 1-16 (1969).